

COMPUTER SIMULATION OF THE LIGHT COLLECTION PROCESS
IN SCINTILLATION GAMMA-RAY CAMERAS

G. Normand, M. Jatteau, P. Lelong and J. Ott

Laboratoires d'Electronique et de Physique appliquee,
3, avenue Descartes, 94450 Limeil-Brevannes, France

ABSTRACT

A computer simulation program based on the Monte Carlo method is presented. The physical model takes into account the main phenomena which occur from the interaction of a gamma quantum with the scintillating crystal to the primary electron emission by the photocathode of photomultiplier tubes closely coupled to the large scintillator plate of the camera head. Computed and experimental results of the mean values as well as the statistical characteristics of signals delivered by the photomultiplier tubes are found to be in good agreement for various camera head configurations. The usefulness of this computer program is shown.

INTRODUCTION

Most of the gamma-ray cameras presently used in Nuclear Medicine to follow the behaviour in vivo of radiopharmaceutical products include a scintillation camera head based on the invention of H.O. Anger^{1,2}. The scintigraphic images obtained with such cameras result from the accumulation of a large number of detected gamma quanta and give information on the spatial distribution of the radioactivity in tissue^{3,4}. In addition to the correction location and shape of radioactive regions, the main feature of the scintigraphic images is the possible evaluation of the local count rates as well as their variations in space and in time. Gamma-ray cameras must be considered not only as imaging systems but also as measuring instruments able to process non scattered gamma photons with a view to estimate the amounts of radioactivity localized in organs of interest.

Significant improvements of scintillation camera performance have been made by introducing technologically advanced components, refinements in pulse handling and more recently micro-computer based

correction systems^{5,6,7}. However, very few publications are devoted to the investigation of the optical components of the camera head^{8,9,10} and the purpose of our study was to establish a simulation program which allows the computer to study the light collection process by PM tubes in scintillation camera heads.

This paper deals with the presentation of this computer program based on the Monte Carlo method and compares simulated and experimental results obtained on various camera head configurations.

COMPUTER SIMULATION PROGRAM

Several computer programs have been developed at LEP with a view to an optimization study of gamma-ray cameras. In particular, the simulation of light collection by the PM tubes in Anger cameras, based on photometric analysis¹⁰ has given results in good agreement with simple experiments. However, a second approach was necessary to be able to take into account some physical parameters such as light attenuation along the different tracks, multiple reflections of light inside the NaI(Tl) crystal itself or on the input and output planes of the optical block. In addition, it was interesting to introduce the statistical aspects related to the main phenomena considered.

This new approach used the statistical properties of the light propagation from the quanta point of view. The track followed by each "blue" photon from the scintillation "point" to its final absorption location is determined. At each interface between two different media the parameters of such a track are computed by means of the Monte Carlo method by using the probability laws defined from the optical properties of the respective media and interfaces.

Physical Model

A scintillation camera head includes in particular a large NaI(Tl) crystal plate, a large diameter optical window so called a "light guide" and a set of PM tubes coupled to the output plane of the light guide as indicated in Figure 1. A part of such an optical block is

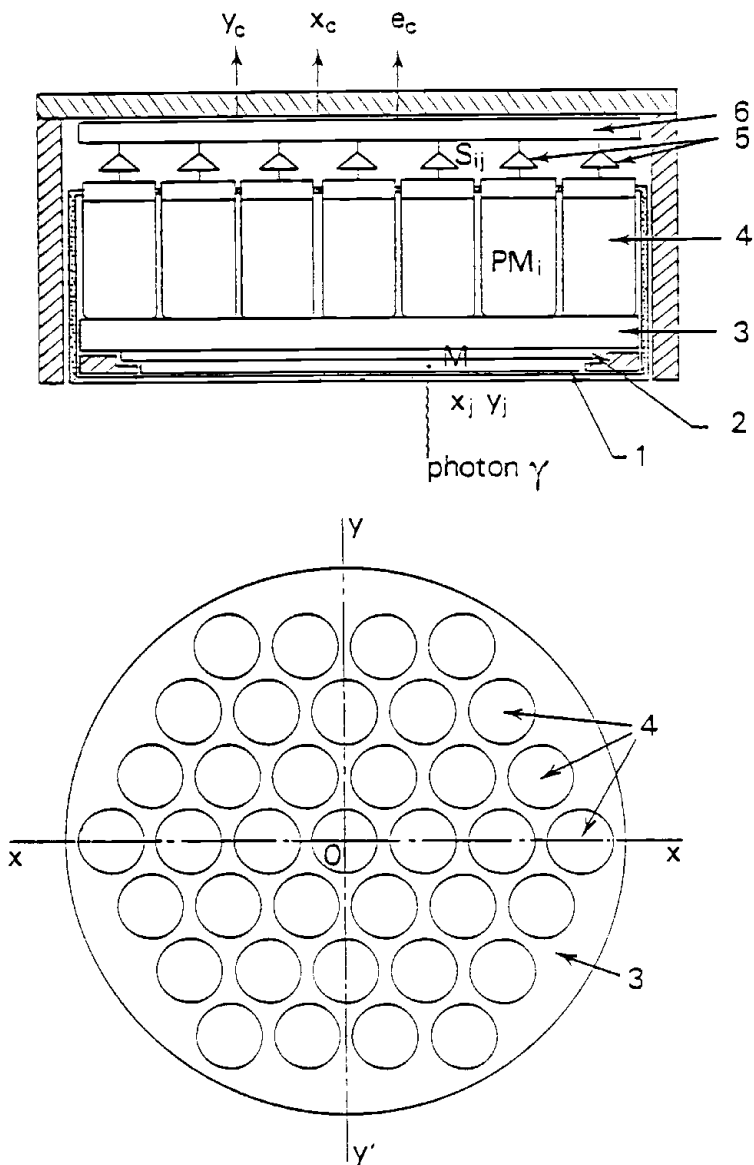


Figure 1. Schematic representation of a scintillation camera provided with 37 photomultiplier tubes. 1. NaI(Tl) crystal; 2. pyrex window; 3. perspex window; 4. PM tubes; 5. data acquisition channels; 6. analog computer delivering coordinates x_c , y_c and e_c of events.

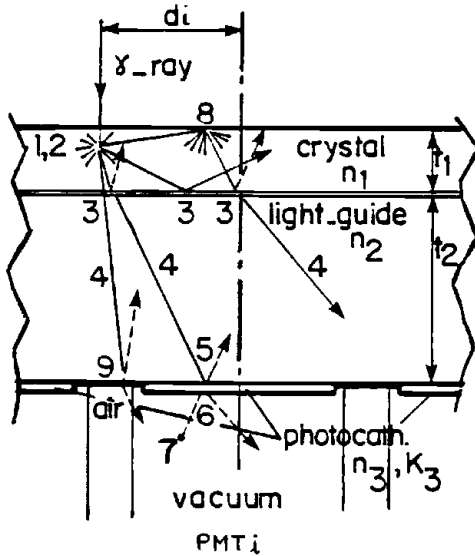


Figure 2. Part of the section of a scintillation camera head illustrating the location of the physical phenomena (1 to 9) taken into account in the computer simulation program.

seen in Figure 2. The main physical phenomena which occur from the interaction of a gamma quantum with the matter (1) to the emission of a primary electron by the photocathode of PM tubes (7) are illustrated in Figure 2. They are briefly described below.

It is assumed that a large number of "observable blue" photons (mean wavelength equal to 410 nm) are emitted from the scintillation "point" (4000 gamma quanta from a 122 KeV CO^{57} source) with an isotropic emission law (2). The location in depth of this scintillation point (1) is related to the linear absorption coefficient of the crystal for the energy of gamma quanta. According to their emission direction the photons can be either transmitted from the NaI(Tl) crystal to the light guide (3,4) and absorbed into the photocathode layer (6)(contributing to "direct light") or reflected either inside the crystal itself (3 or 8) or on the output plane (5 or

9) to reach finally one of the photocathodes (participating to "reflected light"). Because of manufacturing defects, the input plane scatters the light. The optical parameters of these reflections being the "albedo" (directional scatter reflection factor) and the Lambert's reemission law (8). At the "crystal-light guide" interface (3) the photons can be either reflected (probability $P(r)$ equal to the reflection factor deduced from the Fresnel's laws) or transmitted (probability $P(t) = 1 - P(r)$). For a track length L into a given medium (having a linear absorption coefficient μ) the probability of photon absorption (4) is $P(L) = 1 - e^{-\mu L}$. The photons reaching the photocathodes with an incidence angle θ can be either reflected (5) or transmitted (6) or absorbed (7) according to the respective probabilities defined from the optical properties of the photoemissive layer. These properties are computed by means of a sub-program which determines the variations of the reflection, transmission and absorption factors as a function of the incidence angle. Figure 3 shows an example of such curves for a given photoemissive layer corresponding to the bialkali photocathode of PM tubes used in scintillation cameras.

A very simple model for the electron emission from the photocathode (7) is used in our program, the emission probability for each absorbed photon being .45 for this kind of photoemissive layer.

In addition, the photons reaching the output plane outside the photocathode area (9) can be either reflected or transmitted or absorbed according to the properties of the optical treatment of these regions (mirror, scattering layer or free "glass-air" interface can be chosen).

For each scintillation the tracks of photons are successively computed until either absorption or loss towards the borders of the camera field of view (FOV). This process is repeated to simulate in a random manner a large number of scintillations originating from a particular location.

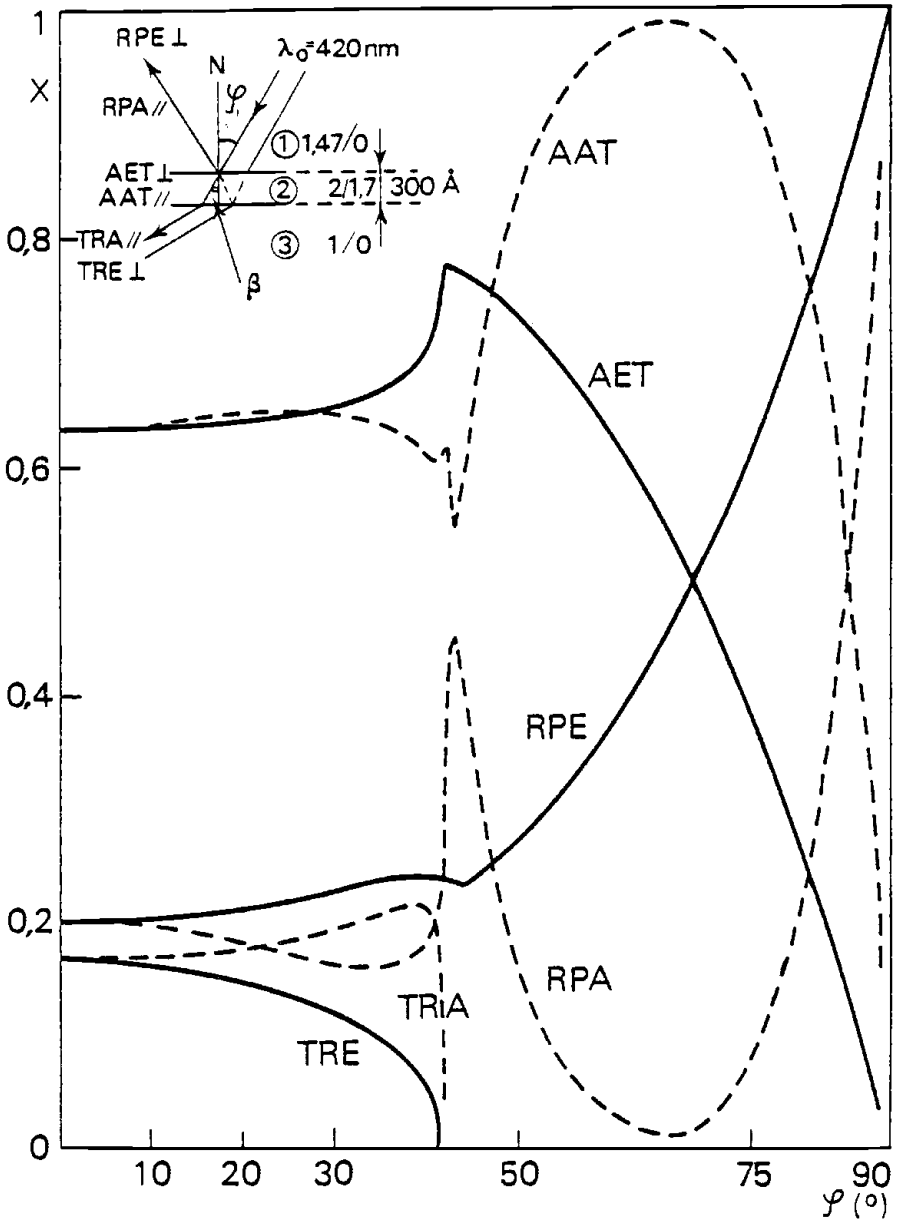


Figure 3. Light propagation and absorption at the PMT photocathode interface of a scintillation camera head. Example of variations of reflection (RPE, RPA), absorption (AET, AAT) and transmission (TRA, TRE) factors from the light guide (1) to the vacuum (2) through the bialkali photoemissive layer (3) in function of the incidence angle (from ref. 10).

Input data and computed results

The geometric and physical parameters of the optical block have to be fixed according to the camera head configuration under consideration. The input data file includes:

- (i) the coordinates of the gamma-ray beam (x,y) and the energy (E) of the gamma quanta.
- (ii) the thickness and refractive index of the scintillating crystal (t_1, n_1) , light guide (t_2, n_2) and photoemissive layer $(t_3, n_3 + ik_3)$ for the mean wavelength corresponding to the scintillation light.
- (iii) the number of PM tubes (P) and their location according to the arrangement over the field of view (such as the one shown in the Figure 1) and the useful (ϕ_{p_k}) and external (ϕ_{ex}) PMT diameters.
- (iv) the reflection factor of the entrance scattering plane (P_e) and that for the area located outside the photocathodes (P_a) with an optional reflection law according to the optical treatment considered.
- (v) the linear absorption coefficients of the crystal, μ_γ for the gamma-ray beam of energy E , μ_c for the scintillation light and that for the light guide μ_g .

Several interesting computed results such as the light distribution over the output plane of the optical block, the "direct" light collected by the PMT photocathodes or the incidence angle distribution of the photon tracks are not easily obtained experimentally. These results are presented in another paper (11). The ones which can be compared to experimental values have been used to verify the computer simulation program and are listed below:

- (i) the numbers of primary photoelectrons $N(d_i)$ emitted by each PMT photocathode i the axis of which is located at a distance d_i from the scintillation point (see Figure 2) are closely connected to the pulse height corresponding to the signal delivered by the PM tube i . These numbers are computed for each simulated scintillation and their mean values, are delivered

$$\overline{N(d_i)} = S^{-1} \sum_j N_j(d_i)$$

from a series of S scintillations j located at the same

address. The program can deliver directly the normalized "signal-distance" curve defined by $F(d) = \overline{N(o)}^{-1} \cdot \overline{N(d)}$ very often used in scintillation camera design.

- (ii) the normalized standard deviation of the S random values of $N(d_i)$ is related to the FWHM energy resolution $R_E(d_i)$ evaluated from the scintillation detection spectrum of the output signals delivered by the PM tube i. The "energy resolution-distance" curve $R_E(d)$ is also directly computed by the program.
- (iii) the random fluctuations of the total number of electrons emitted by all the P photocathodes ($\sum_{i=1}^P N(d_i)$) can be characterized by the distribution diagram of the S computed values or by the corresponding standard deviation. This latter is closely related to the FWHM energy resolution of the camera, R_{EC} .

Experimental verifications and discussion

Experimental verifications have been performed by comparison of the computed results with the measured ones on a laboratory model of an Anger camera head. This unit is provided with a NaI(Tl) crystal plate (thickness $t_1 = 6$ mm; diameter = 30 cm) coupled to a pyrex window (thickness $t_W = 9$ mm; diameter = 40 cm)*, with an additional perspex window (thickness t_A ; diameter = 40 cm) and with a set of 37 x 2" PM 2102 photomultiplier tubes**. The corresponding light guide thickness is $t_2 = t_W + t_A + 4$ mm (taking into account the thickness of PMT front windows and the coupling media) which has been varied in our experiments from 13 mm to 29 mm by means of different perspex windows.

The test bench used for experimentation is represented in Figure 4. A narrow gamma-ray beam emitted by a well collimated CO^{57} point source scans the camera field of view (FOV) by means of an XY scanning table according to a given track pre-programmed on the P855 mini-computer. Acquisition of PMT output signals is made by a multi-channel analyzer after amplification and pulse shaping and, from the scintillation detection spectrum recorded for a given PMT located at

* Harshaw Chemie BV, De Meern, Holland

** RTC, Paris, France

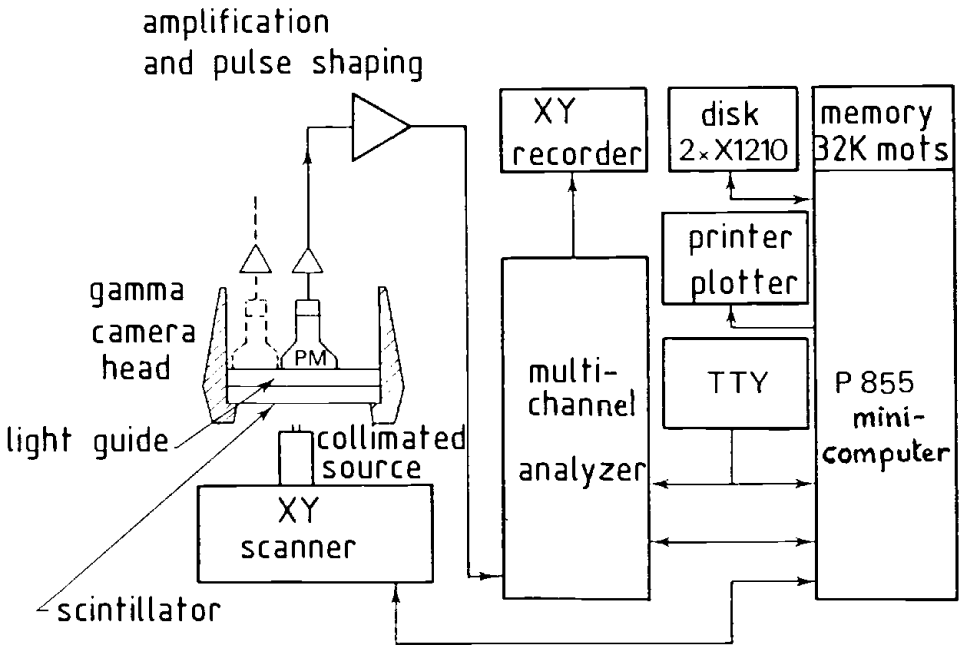


Figure 4. Block diagram of the test bench used for the experimental study of the light collection process.

the distance from the gamma-ray beam, the mean value $S(d)$ and energy resolution $R_E(d)$ are deduced by using data processing performed in the mini-computer. In fact, several such measurements according to different symmetry axes of the photocathode are made and the experimental "signal-distance" curves result from the averaging of the measured values for the same distance d .

In Figure 5 computed and measured curves are plotted for $t_1 = 6$ mm and $t_2 = 19$ mm (i.e. $t_A = 6$ mm in the camera model). Similar results are presented in Figures 6 and 7 as a function of the light guide thickness. The scale of $S(d)/S(0)$ is chosen according to the distance d in order to enhance the small differences between measured and computed values. In each case, the maximum relative error is given.

Although some optical parameters not very well known had to be determined from successive experiments, a very good agreement between computed results and experimental ones is found for a large range of

○, Δ : meas. — : comp.

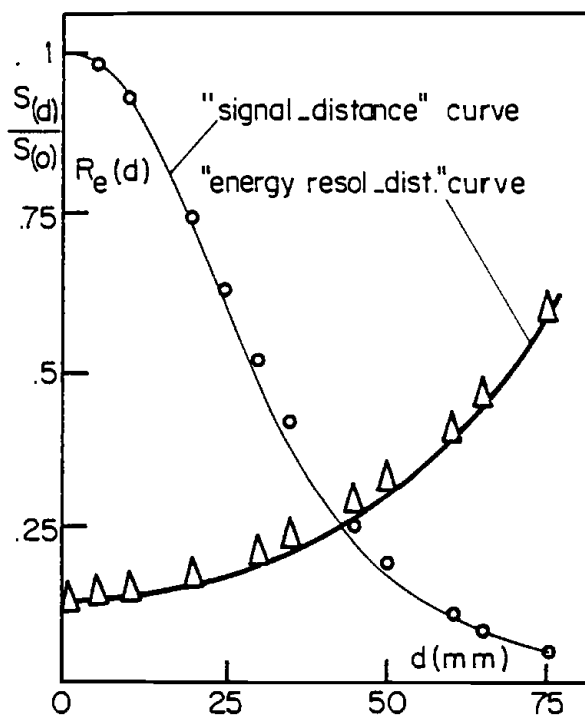


Figure 5. Comparison between computed and measured results for the laboratory model of gamma camera.

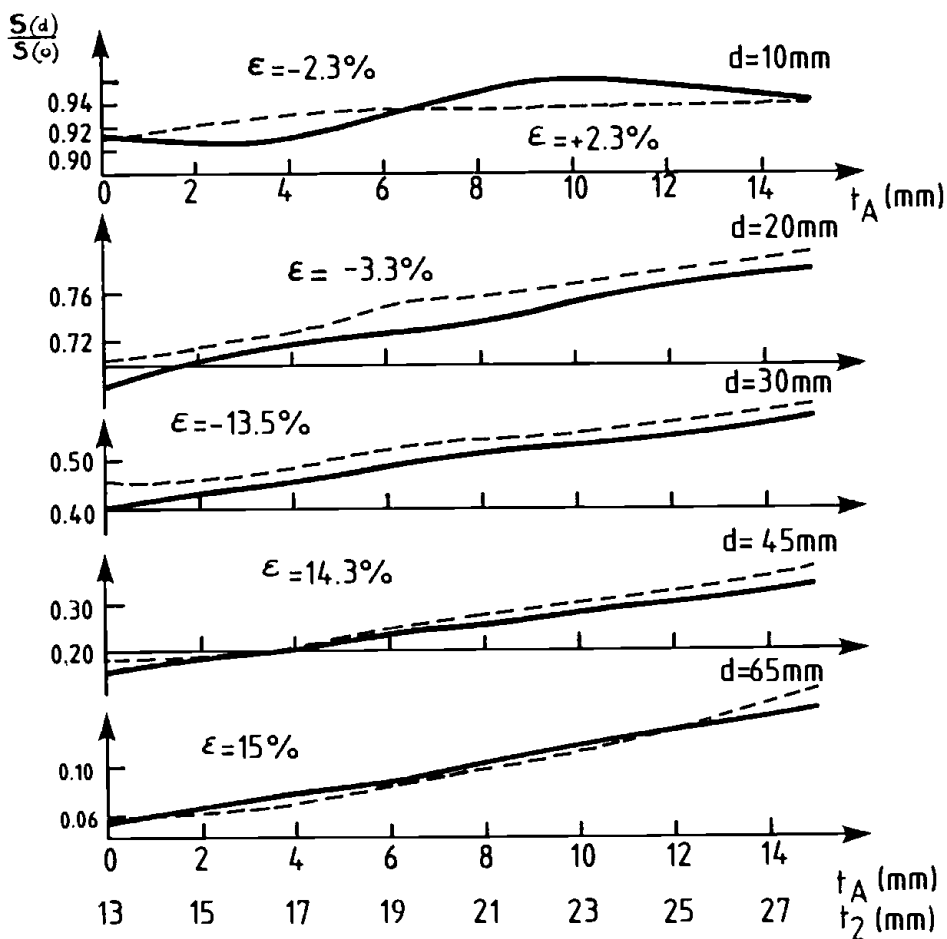


Figure 6. Computed (—) and measured (----) variations of the normalized PMT output signals in function of the light guide thickness (t_2) at various distances (d) "scintillation-PMT axis".

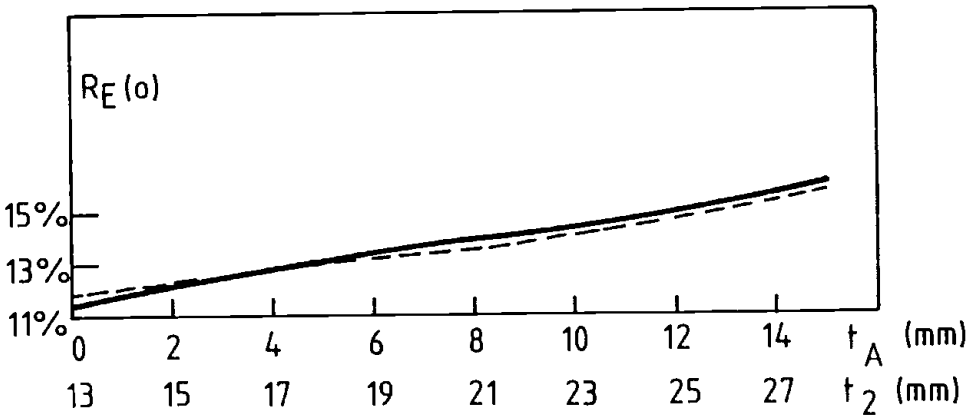


Figure 7. Computed (—) and measured (----) FWHM energy resolution for $d = 0$ in function of the light guide thickness (t_2).

distance d as well as for numerous light guide thicknesses. The agreement is valuable for mean values as for the energy resolutions which characterize the statistical processes. In addition, good agreement is also found with the results of the previously developed computer simulation (10) which could be used in the case of simplified camera head configurations including only the central PM tube coupled to the optical block.

CONCLUSION

The good agreement obtained between computed and experimental results for various camera head configurations confirms that the computer simulation presented in this paper is very close to the real light collection process in scintillation cameras. This program allows the study of some particular phenomena which cannot be easily observed experimentally (11). It can be used with confidence for an optimization study of scintillation cameras.

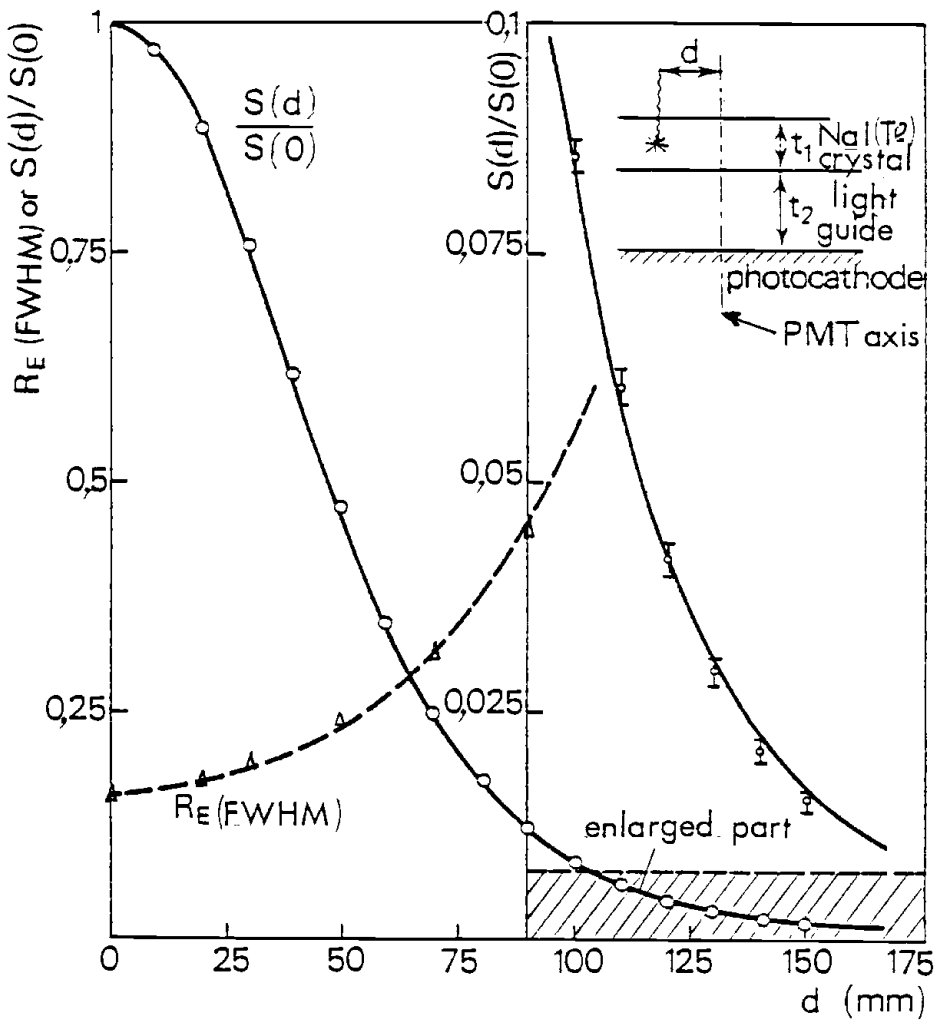


Figure 8. Comparison between computed and measured (o,Δ) results for a simplified camera head ($t_1 = 12.5$ MM; $t_2 = 32$ MM; 3 inch x P 2030 PMT) (From Ref 10).

ACKNOWLEDGEMENTS - We wish to thank Mr. J. Houdard for his participation to the computer study of optical properties of multiple layers.

REFERENCES

1. H.O. Anger, "Scintillation camera", Rev. Sci. Instruments 29, 27-33, 1958.
2. H.O. Anger, "Sensitivity and resolution of the scintillation camera" in "Fundamental problems in scanning", A. Gottschalk and R. Beck (eds.), Springfield, Ch. C. Thomas, 117-144, 1968.
3. R.N. Beck, "The scanning system as a whole" in "Fundamental problems in scanning", A. Gottschalk and R. Beck (eds.), Springfield, Ch. C. Thomas, 17-39, 1968.
4. G.J. Hine and J.A. Sorenson, "Instrumentation in Nuclear Medicine", Vol. 1 and 2, Academic Press, New York, 1974.
5. G.J. Hine and P. Paras, "Performance of scintillation cameras", J. Nucl. Med., 16, 1206-1207, 1975.
6. R.E. Zimmerman, "Advances in nuclear medicine imaging instrumentation" in "Medical Radionuclide Imaging", Vienna IAEA, Vol. 1, 121-139, 1977.
7. G. Muehllehner and J. Colsher, "Single Photon Imaging, new instrumentation and techniques" in "Medical Radionuclide Imaging", 1980; Vienna IAEA, Vol. 1, 173-198, 1981.
8. J.W. Scimger and R.G. Baker, "Investigation of light distribution from scintillations in a gamma camera crystal", Phys. Med. Biol., 12, 101-103, 1967.
9. J.B. Svedberg, "On the intrinsic resolution of a gamma camera system", Phys. Med. Biol., 17, 514-524, 1972.
10. M. Jatteau, P. Lelong, G. Normand, J. Ott, J. Pauvert and J. Pergrale, "Pour une optimisation des cameras de gammagraphie de type Anger", Acta Electronica, 22, 2, 91-117, 1979.
11. M. Jatteau and G. Normand, "Influence of optical and geometrical parameters on scintillation detection in gamma camera heads" in "Advances in Scintillation Counting", S.A. McQuarrie, C. Ediss and L.I. Wiebe (Eds), University of Alberta Press, Edmonton, p. 190-207, 1983.